EFDA–JET–PR(11)05

V.G. Kiptily, S.D. Pinches, S.E. Sharapov, B. Alper, F.E.Cecil, D. Darrow,
V. Goloborod'ko, A.W. Morris, C. Perez von Thun, V. Plyusnin, V. Yavorskij,
T. Craciunescu, M. Gatu Johnson, C. Hellesen, T. Johnson, H. R. Koslowski,
J. Mailloux, F. Nabais, M. Reich, P. de Vries, V.L. Zoita
and JET EFDA contributors

Studies of MHD Effects on Fast Ions in JET

Studies of MHD Effects on Fast Ions in JET

V.G. Kiptily[1], S.D. Pinches[1], S.E. Sharapov[1], B. Alper[1], F.E.Cecil[2], D. Darrow[3], V. Goloborod'ko[4,5], A.W. Morris[1], C. Perez von Thun[6], V. Plyusnin[7], V. Yavorskij[4,5], T. Craciunescu[8], M. Gatu Johnson[9], C. Hellesen[8], T. Johnson[10], H.R. Koslowski[11], J. Mailloux[1], F. Nabais[7], M. Reich[6], P. de Vries[12], V.L. Zoita[9]
and JET EFDA contributors*

JET-EFDA, Culham Science Centre, OX14 3DB, Abingdon, UK

[1]*EURATOM-CCFE Fusion Association, Culham Science Centre, OX14 3DB, Abingdon, OXON, UK*
[2]*Colorado School of Mines, 1500 Illinois Street, Golden, CO 80401, Colorado, USA*
[3]*Princeton Plasma Physics Laboratory, Princeton, NJ 08543, New Jersey, USA*
[4]*EURATOM/OEAW Association, Institute for Theoretical Physics, University of Innsbruck, Austria*
[5]*Institute for Nuclear Research, Kiev, Ukraine*
[6]*Association EURATOM-FZ Jülich, Institut für Energieforschung - Plasmaphysik, Germany*
[7]*Association Euratom/IST, Instituto de Plasmas e Fusão Nuclear, Lisboa, Portugal*
[8]*EURATOM-MedC Association, National Institute for Laser, Plasma and Radiation Physics, Romania*
[9]*Association EURATOM-VR, Department of Physics and Astronomy, Uppsala University, Sweden*
[10]*Association EURATOM –VR, Royal Institute of Technology KTH, Stockholm, Sweden*
[11]*EURATOM/MPI für Plasmaphysik Association, Garching, Germany*
[12]*FOM institute for Plasma Physics Rijnhuizen, Association EURATOM-FOM, the Netherlands*
** See annex of F. Romanelli et al, "Overview of JET Results",*
(23rd IAEA Fusion Energy Conference, Daejon, Republic of Korea (2010)).

Preprint of Paper to be submitted for publication in
Nuclear Fusion

ABSTRACT.
Fast ion behaviour is central to burning plasma physics, auxiliary heating and current drive, and losses can cause significant plasma-wall interactions. Here fast ion losses on JET caused by plasma disruptions, TAE, fishbones are described. There are now several relevant diagnostics on JET: gamma-ray diagnostics, NPA, neutron spectrometry, Faraday Cups and a Scintillator Probe were used for simultaneous measurements of various species of confined and lost fast ions in the MeV energy range. The fast ion populations were generated in fusion reactions and were also produced by NBI and by accelerating with ICRH. Fast ion losses preceding disruptions were often detected by the Scintillator Probe in discharges with high β_N. It was found that the losses are caused by the m = 2/n = 1 kink mode and these losses typically occur at the same time as the thermal quench, before the current quench that follows. A set of experiments was carried out where interactions of core-localised TAE modes with fast ions in the MeV energy range were studied in plasmas with monster sawteeth. Energy and pitch angle resolved SP measurements of MeV-ions ejected from the plasma due to fishbone oscillations driven by NBI-ions are also studied.

1. INTRODUCTION

Studies have been performed on JET of fast ion losses caused by plasma disruptions, TAE and fishbones. This work is carried out as continuation of fast ion research on JET [1] due to its significance for the future JET operation with ITER-like beryllium wall, and uses the improved diagnostic capability built up on JET in recent years. Understanding loss of fast ions is likely to play a crucial role for the design of plasma facing components for DEMO and for operation of ITER.

Gamma-ray diagnostics [2,3], neutral particle analyser (NPA) [4], neutron spectrometry with TOFOR [5], Faraday Cups [6] and Scintillator Probe (SP) [7] were used for simultaneous measurements of various species of confined and lost fast ions in the MeV energy range in D, D-^{3}He, and D-^{4}He plasmas. The high time resolution of diagnostics allowed the study of both resonant and non-resonant MHD effects on redistribution and losses of energetic ions, e.g. whether modes resonant with one part of the fast ion distribution strongly affect other (non-resonant) parts. The fast ion populations were generated in fusion reactions D+D$\rightarrow$p(3MeV)+T(1MeV), D+^{3}He$\rightarrow\alpha$(3.7MeV)+p(15MeV), and were also produced by NBI and by accelerating minority-ions or NBI-ions with ICRH. The losses from the three types of instability are described in turn, providing an overview of recent work as well as new results.

2. FAST ION LOSSES AND DISRUPTIONS

Fast ion bursting losses preceding a plasma crash or disruption were detected by SP in Advanced Tokamak (AT) plasma discharges with high β_N and q(0)>1.5 [8]. m = 2/n = 1 infernal kink modes and m = 3/n = 2 NTMs were dominantly limiting plasma performance in these experiments. The most significant impact on the plasma was in the case of the m = 2/n = 1 modes with high amplitudes. Figure 1 shows time traces of electron temperature, the n = 1 MHD signal, internal plasma inductance, plasma current, toroidal rotation and fast ion losses measured with an array of photomultipliers observing the scintillator plate for two Pulse No's: 77894 and 77896 with a weak internal transport barrier.

In these discharges MHD activities rather similar in structure (magnetic spectrograms shown on Fig.2.) are leading to different consequences depending on their size. In the first discharge (Pulse No: 77894), one can see a fast drop of T_e. In the second one this MHD instability initiates a thermal quench with a disruption following.

A theory of fast ion redistribution due to m = 2/n = 1 kink-mode instability has been developed in Ref.9, where the interaction mechanism of energetic trapped ions with the pressure driven MHD instability similar to that shown in Fig.1 was studied, but without SP data. As in [9] it was found that due to the mode there is an abrupt change of the internal inductance. In the case of discharge with disruption (Pulse No: 77896) the internal inductance and plasma rotation are dropping down similarly to [9] just before the thermal quench. In the Pulse No: 77894 the plasma rotation also decreases though an increase in inductance was observed. One notes that in the Pulse No: 77894 the plasma rotation was significantly decreased off axis at R = 3.3-3.4m during the crash (t_{cr} = 5.533s), while a central plasma rotation drop was observed in the case on Pulse No: 77896 (t_{cr} = 5.485s). Rotation changes can change the interaction with the precessing fast ions. Figure 3 demonstrates how the electron temperature profile reacts on the MHD events in these shots. Location of the mode at the q = 2 is seen from the changes in the electron temperature profiles.

The magnetic reconnection may affect energetic trapped ions and direct evidence of this comes from the losses observed with SP shown on Fig.4. The detected ions are assumed to be lost due to small changes in Larmor radius or pitch angle of confined ions, i.e. that the Larmor radius and pitch angle measured at the probe are very close to those if the ion before it was scattered onto the lost orbit. There is no evidence provided by the γ-ray spectrometers that the D-beam ions were accelerated by the ICRF (i.e. γ-ray emission from the $^{12}C(D,p\gamma)^{13}C$ reaction was not detected), showing it is reasonable to interpret the SP signal as due to ICRH accelerated H-ions only. The losses observed in the quiescent period before the reconnection in Pulse No: 77894 at t = 5.475s are primarily around the trapped-passing boundary in phase space. Similar losses are seen in the period without MHD at t = 5.425s in Pulse No: 77896. The footprints of losses at t = 5.525s (Pulse No: 77894) and t = 5.475 (Pulse No: 77896) are covering the crash (Pulse No: 77894) and the whole disruption period (Pulse No: 77896). The saturation of the MHD signal in Fig.1 prevents the investigation of the loss intensity as function of the mode amplitude in this case. However the temporal evolution of the losses detected by SP shows the phase space of the losses moves notably during the reconnection. During the crash in Pulse No: 77894 the main losses are around the pitch angle of ions resonant with the RF, deeper in the trapped region: the pitch-angle of the maximum loss is on the red line which is related to ICRF resonance position on the SP grid. The pitch-angles of resonant H ions detected by SP lie at pitch angle $\theta \cong \arccos(1-R_{res}/R_{SP})^{1/2} = 60^o$, with $R_{res} \cong 2.90$m and $R_{SP} = 3.82$m being correspondingly major radii of the resonance and the scintillator probe. For the disruption in Pulse No: 77896 a similar trend is seen, but the loss region is very much expanded and the total losses much higher, as a consequence of the much larger instability/reconnection and probably more complex magnetic structure, but interestingly still localised to a small part of phase space (at the SP location). After the event in Pulse No: 77894, the quiescent losses are reduced (Fig.4 (a), 3rd frame), suggesting the fast ion population has been significantly depleted.

The orbits of lost H-ions calculated backward in time from the different hot spot coordinates, (9cm, 57^{o}), (9cm, 58^{o}) and (7cm, 59.5^{o}) are presented in Fig.5, changing from marginally passing to trapped (as above, the lost ions are assumed to be scattered from neighbouring confined orbits).

3. FAST ION INTERACTION WITH TORNADO MODES

A set of experiments were carried out where interactions of core-localised TAE modes [11, 12], so-called 'tornado' modes localised inside the q = 1 magnetic surface, with fast D-ions in the MeV energy range were studied in plasmas with monster sawteeth.

The tornado modes were identified as core-localized TAEs within the q = 1 radius [13]. The effect of tornado modes on fast particles has been first detected on JT-60U [11], where a significant loss of the fast-ion confinement and degradation of total plasma energy content were observed. Also TAE and tornado mode activities affecting fast ion power deposition profiles were found on DIII-D [14, 15] and on TFTR [16]. The fast particle redistribution/ losses similar to these observed on JT-60U were found on JET as a significant (by a factor of 2) decrease of γ-ray emission coming from the nuclear reaction $^{12}C(p,p'\gamma)^{12}C$ during the combined activity of tornado modes (inside the q = 1 radius) and TAE (outside the q = 1 radius) [17,18]. Also core-localized TAE modes were observed to cause significant fast ion redistribution in the plasma core and enhanced losses in AT plasma discharges [19]. This is a resonant process, and it is estimated that deuterons with energy ~0.5MeV are resonant with the tornado modes.

Measurements of confined fast particles with 2D γ-ray camera allowed distinguishing the energy ranges of fast D-ions using γ-ray emission from the $^{12}C(D,p\gamma)^{13}C$ reaction threshold deuteron energy $E_D \approx 0.5$MeV [3], a much lower threshold than the 4.5MeV proton threshold of the $^{12}C(p,p,\gamma)^{12}C$ reaction in [17,18]. In addition DD neutron data from the TOFOR provides information on high energy deuterons $E_D > 0.5$MeV [5]. This allows observing their spatial redistribution during the core-localised TAE activity preceding monster sawtooth crashes.

In the present JET experiments a population of the fast particles was obtained by central 3rd harmonic ICRF heating of D-beam ions. A similar scenario has been used in experiments where ^{4}He beam ions were accelerated in ^{4}He-plasmas [3]. Figure 6 shows wave-forms of a typical plasma discharge with a monster sawtooth. The tornado modes, one sees from Fig.7, showing a spectrogram made with a fast magnetic probe, are represented by many discrete modes. Just before the crash, at t>15.1 sec the following toroidal mode numbers of TAE and bi-directional tornado modes are seen with toroidal mode numbers n = 3, ±4, ±5, 6, 7, 8. The existence of the n = 3 mode, the lowest-n mode before the monster sawtooth crash, shows that q (0) at the time of the mode appearance, 15.1

sec, has to be below $q_{TAE}^{n=3} < 0.8$, i.e. the existence condition, (2m+1)/2n, for n = 3.

In all discharges with tornado modes an extensive re-distribution of fast D-ions in the energy range of 0.8MeV – 1.8MeV was observed with 2-D γ-camera. Indeed, line-integrated emissivities of 3.1MeV γ-rays from the $^{12}C(D,p\gamma)^{13}C$ reaction depicted on Fig.8 show that intensities of central channels of the vertical camera (#15 and #16) begin slowly decreasing with appearing tornado modes during the monster sawtooth period. At the same time, intensities of the high- and low-field side channels (#14, #17 and #18) are growing up. That means the energetic particles are leaving the plasma centre and moving toward the periphery. The lines of sight for neutron and γ-spectrometers are relatively narrow and are overlapping with γ-ray camera channels #14, #15 and ch#16. Neutron and γ-ray spectrometry have also provided evidence of the D-ion redistribution [5]. It was found that intensity of DD-neutrons with energy $E_n > 4.5$MeV produced by ions with $E_D > 1.3$MeV is decreasing in the period of the tornado mode development. The same tendency has been observed for 3.1MeV gammas from the $^{12}C(D,p\gamma)^{13}C$ reaction measured in the TOFOR field of view.

One can see that at around t = 15.5s the observed TAE activity is abruptly terminated by the occurrence of a monster sawtooth crash, which may have been triggered by the loss of fast ion stabilization due to the tornado modes [14-18]. A burst of fast ion losses during the sawtooth crash is clearly seen in Fig.6. The change in the equilibrium profiles as a result of the sawtooth crash, most notably the safety factor, q, then violates the existence criterion for the tornado modes accounting for their abrupt disappearance. The modelling of D-ion redistribution in the presence of tornado modes [20] has been carried out with HAGIS [21] using HELENA [22] equilibrium and TAE modes obtained with CASTOR code [23].

4. FISHBONE EFFECT ON FAST ION LOSSES

Interaction of fusion-born α-particles with fishbones is one of the important issues for burning plasma in ITER-type machine. Estimates show that fishbones may be driven by resonant interaction with relatively low-energy alphas, E ≅ 400keV. For this energy range, any radial transport of the almost thermalised alphas caused by the fishbones may become beneficial since it helps solving the ash removal problem. However, the problem exists whether the low-frequency fishbone driven by thermalised alphas, may also deteriorate the confinement of alphas at much higher energies. This question was discussed in [24], and it was shown that the loss of toroidal symmetry caused by the n=1 perturbation may affect indeed the highly energetic non-resonant alphas strongly. In order to validate the theory of the non-resonant losses, JET experiments were performed for measuring losses of highly energetic ions in the MeV energy range in the presence of the fishbones driven by NBI ions with energy 80 – 100keV. Namely, the energy and pitch angle resolved SP measurements of MeV ions ejected from the plasma during to the non-resonant fishbone oscillations were studied [25]. The lost ions are identified as fast protons accelerated by ICRH (~0.5 – 4MeV). Losses arriving at the probe are enhanced by about a factor 10 – 20 with respect to MHD-quiescent levels, and are found to increase quadratically with the fishbone amplitude. Numerical simulations have been performed which combine the HAGIS, MISHKA and SELFO codes [26]. The losses are found to originate from orbit stochastic diffusion of trapped protons near the plasma boundary or/and from counter-passing protons deep in the plasma core which transit under the influence of the fishbone into an unconfined trapped orbit. The simulations show that the losses are of non-resonant type indeed confirming the mechanism proposed in [24] for highly energetic α-particles.

CONCLUSIONS

In JET discharges with high β_N and q(0)>1.5, the m = 2/n = 1 kink modes limiting the plasma performance were also found to affect strongly the losses of ICRH-accelerated energetic ions. These losses exhibited bursting temporal evolution achieving the peak values (as measured at the SP position) up to factor ~ 20 higher than these in MHD quiescent plasmas. One of the unexpected features for the losses of ICRH accelerated ions during plasma disruptions caused by the kink modes was the preserved pitch-angle distribution of the lost ions. This distribution remained close to the pitch-angle determined by ICRH well after the disruption even though it might be expected that Coulomb collisions could transform the distribution function into an isotropic one. The increase of the losses in amplitude and the narrow pitch-angle of the lost ions may require a further assessment of the impact of such losses on Be wall.

Experiments on beam acceleration with 3rd harmonic ICRH carried out on the JET tokamak provided important new data on the monster sawteeth stabilisation by fast ions interacting with tornado modes (TAE inside the q = 1 radius). In general, the experimental results show trends expected from theory [14-16], which explains the monster crash as a result of the tornado modes expelling fast ions to the region outside the q = 1 radius with the inevitable loss of the fast ion stabilising effect for the sawtooth. This extends earlier studies of this effect on JET [12, 17, 18], with a different fast ion population (deuterium instead of hydrogen) and new γ-ray data on fast ions with energy ≥ 0.5MeV, which is close to the resonance energy for the ion interaction with tornado modes. This allows one to perform the γ-ray "marking" of the fast ions resonating strongly with the tornado modes at the energy range 0.8 MeV−1.2 MeV inside the q = 1 radius. Together with the neutron spectrometry available for D-D reactions, much better coverage of the fast ion redistribution by the tornado modes was experimentally obtained. These experiments provide a very good foundation for the sawtooth and tornado modelling being performed [20].

The experimental observation of the non-resonant losses of trapped energetic ions in the presence of NBI-driven low-frequency fishbones [25] was found to be in line with the theory [24]. This effect could be important for fusion-born alpha-particles in scenarios with fishbones (e.g. hybrid scenarios).

ACKNOWLEDGMENTS.

This work, part-funded by the European Communities under the contract of Association between EURATOM and CCFE, was carried out within the framework of the European Fusion Development

Agreement. The views and opinions expressed herein do not necessarily reflect those of the European Commission. This work was also part-funded by the RCUK Energy Programme under grant EP/I501045.

REFERENCES

[1]. KIPTILY, V.G. et al., Nuclear Fusion **49** (2009) 065030.
[2]. KIPTILY, V.G., et al., Nuclear Fusion **42** (2002) 999.
[3]. KIPTILY, V.G., et al., Nuclear Fusion **45** (2005) L21.
[4]. AFANASYEV, V. I. et al., Review of Scientific Instruments **74** (2003) 2338.
[5]. HELLESEN, C. et al., Nuclear Fusion **50** (2010) 022001.
[6]. DARROW, D. S., et al., Review of Scientific Instruments **75** (2004) 3566.
[7]. BAUMEL, S., et al., Review of Scientific Instruments **75** (2004) 3563.
[8]. MAILLOUX, J., et al., paper EXC/1-4, this conference
[9]. GORELENKOV, N.N. et al., Physics of Plasmas **10** (2003) 713
[10]. PLYUSNIN V. et al., 11st TCM IAEA, Kiev, 2009
[11]. SAIGUSA M. et al., Plasma Physics and Controlled Fusion **40 (**1998) 1647
[12]. SANDQUIST et al., Physics of Plasmas **14** (2007) 122506
[13]. KRAMER G.J. et al., Physical Review Letters **92 (**2004) 015001
[14]. HEIDBRINK W.W. et al., Nuclear Fusion **39 (**1999) 1369
[15]. BERNABEI S. et al., Nuclear Fusion **41 (**2001) 513
[16]. BERNABEI S. et al., Physical Review Letters **84 (**2000) 1212
[17]. PINCHES S. D. et al., Plasma Physics and Controlled Fusion **46** (2004) B187
[18]. SHARAPOV S.E. et al., Nuclear Fusion **45** (2005) 1168
[19]. NABAIS F. et al., Nuclear Fusion **50** (2010) 084021
[20]. GASSNER T. et al., paper in preparation.
[21]. PINCHES S.D. et al Computer Physics Communications **111** (1998) 133
[22]. KERNER W. et al 1998 Journal of Computational Physics 142 271
[23]. HUYSMANS G. T. A., GOELDBLOED J. P., and KERNER W., *Proc. CP90 Conf. Computational Physics*, Amsterdam, the Netherlands, September 10–13, 1990, p. 371, World Scientific Publ. Co.(1991)
[24]. COPPI B., PORCELLI F., Fusion Technology **13** (1988) 447
[25]. PEREZ VON THUN et al., Nuclear Fusion **50** (2010) 084009
[26]. HEDIN J. et al., Nuclear Fusion **42 (**2002) 52

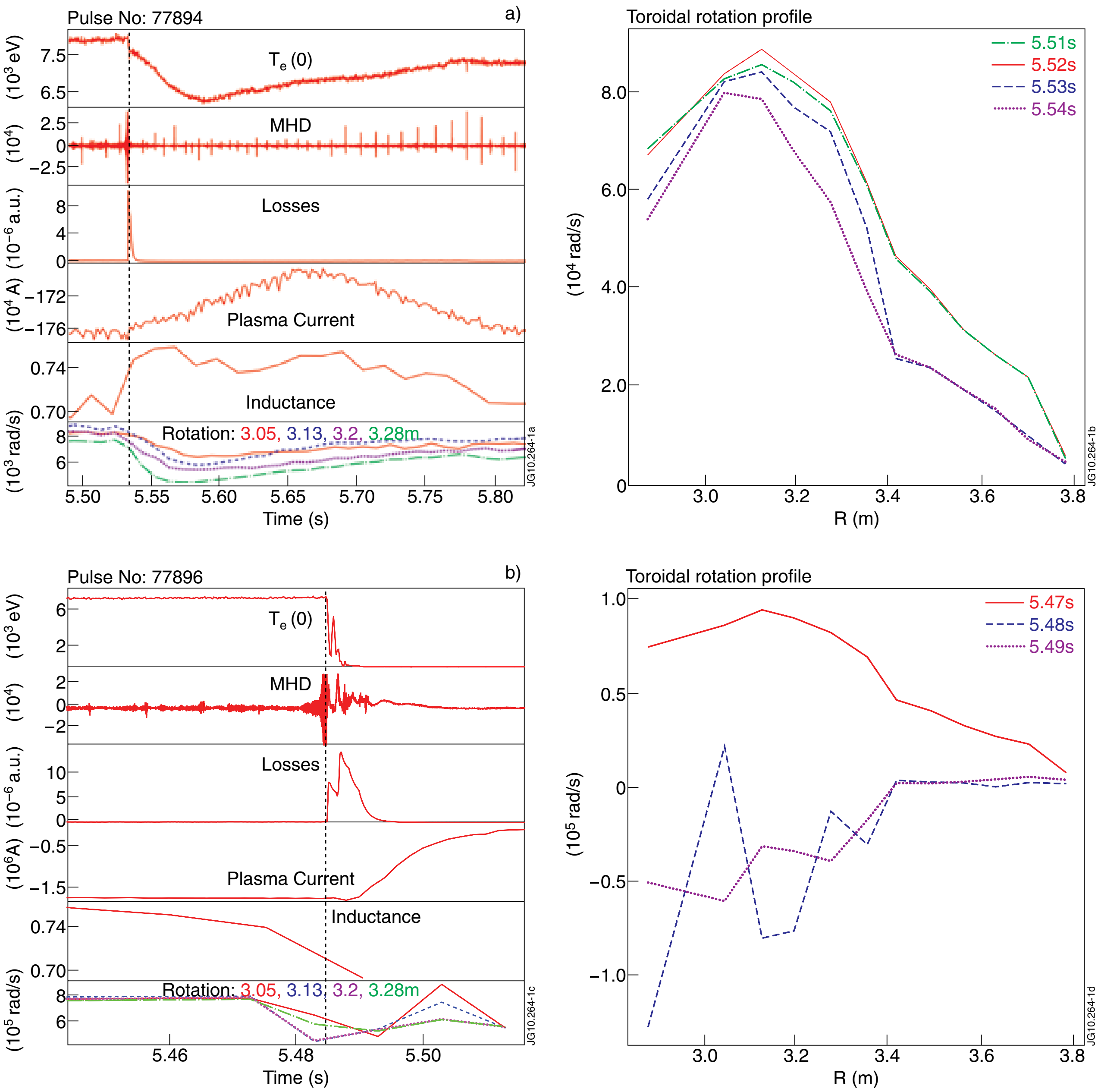

Figure 1: Time-traces of plasma parameters, SP losses and toroidal rotation profiles measured in 2.7T/1.8MA discharges Pulse No's: 77894 (a) and 77896 (b). The fast ion loss waveform is distorted due to saturation of some of the photomultipliers in (b).

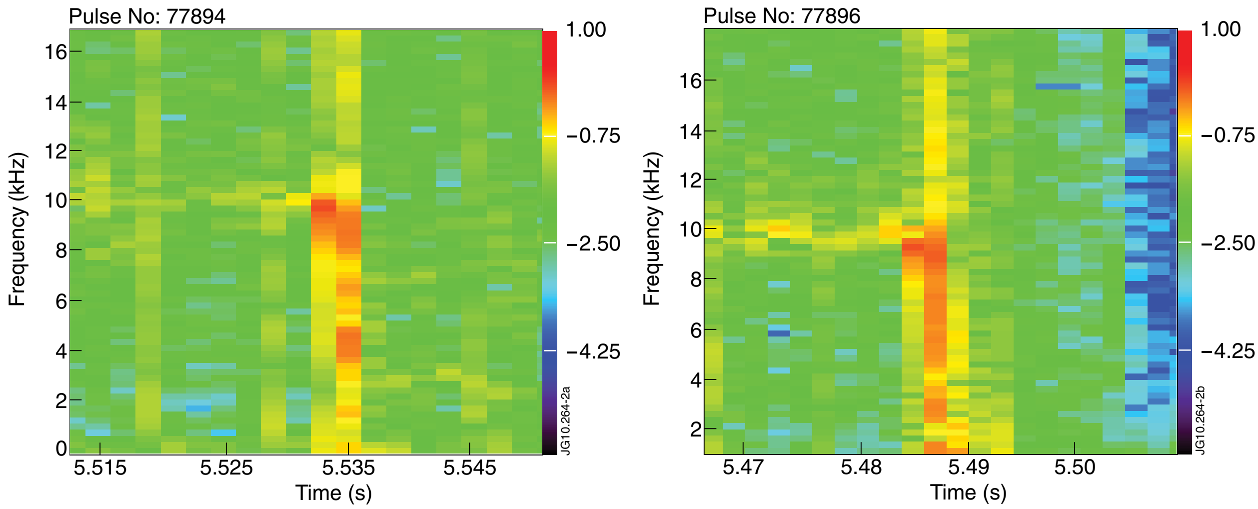

Figure 2: Magnetic spectrograms showing m=2/n=1 mode in Pulse No's: 77894 and 77896.

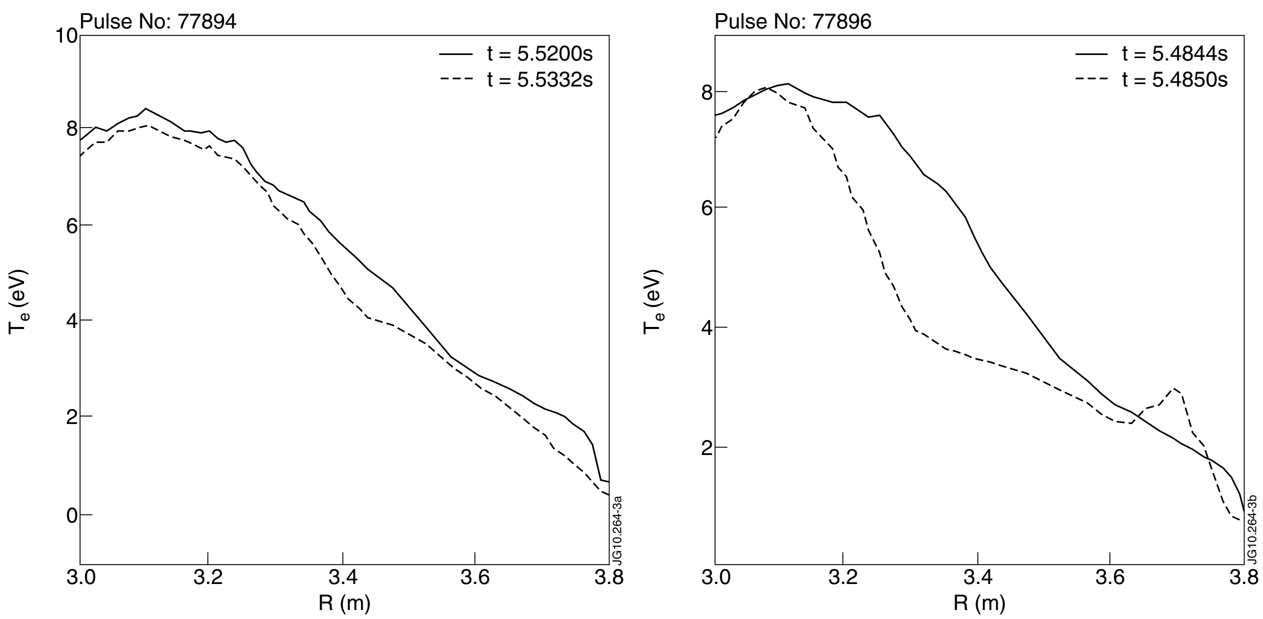

Figure 3: Electron temperature profiles before (solid) and after the crash event (dash) in Pulse No's: 77894 and 77896; before and during MHD q=2 is located at R=3.4m in Pulse No's: 77894 and R=3.3m in 77896.

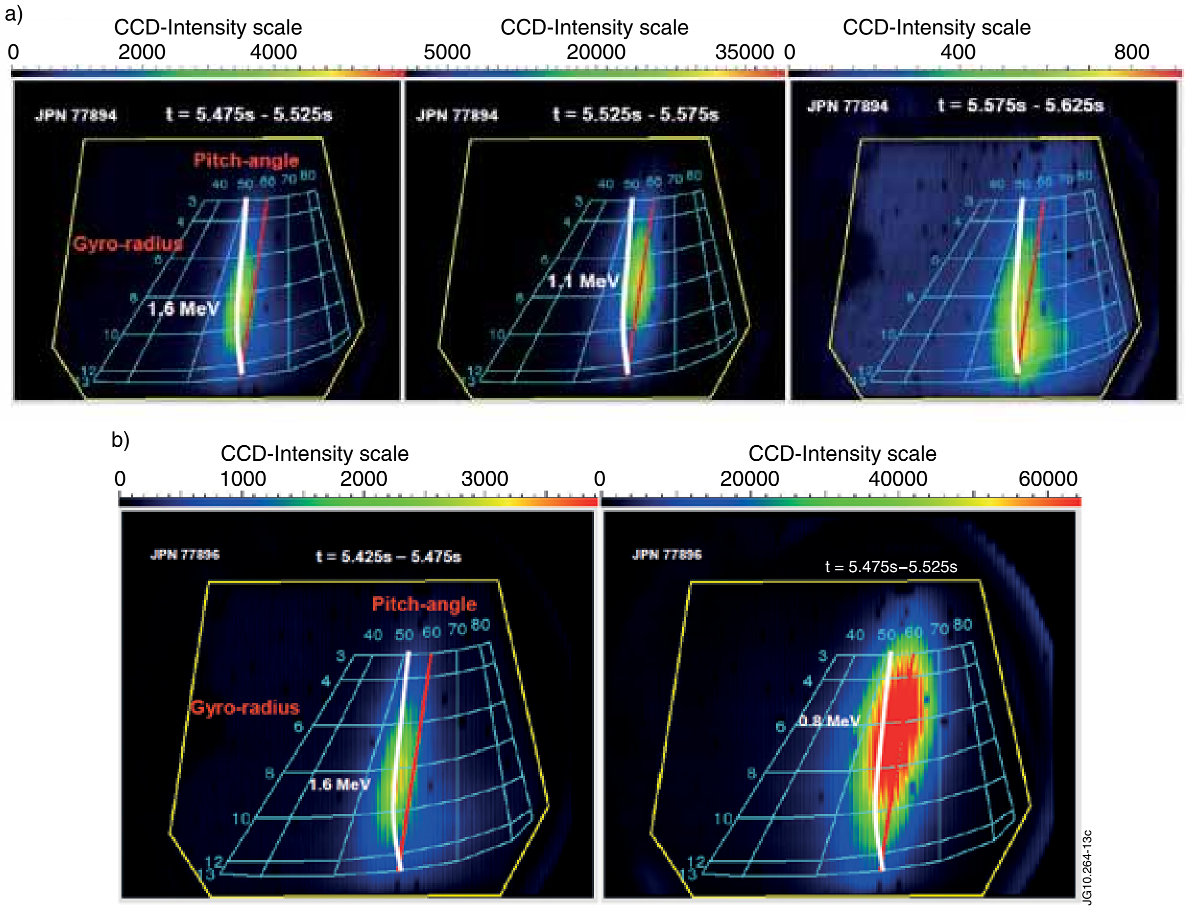

Figure 4: Footprints of losses detected with SP probe: (a) Pulse No's: 77894 with crash at t=5.53s; (b) Pulse No's: 77896 ended with disruption at t=5.486s; exposure of the snapshots – 50ms; red line – pitch-angle of the ICRH resonant ions; white line – the trapped-passing boundary on the SP grid. In (a) and (b) the first footprints related to periods before the crash (Pulse No's: 77894) and the disruption (Pulse No's: 77896); massive losses during the crash (second upper footprint) and the disruption (second footprint in the bottom) are clearly seen. The losses after the crash are shown in (a,) third footprint.

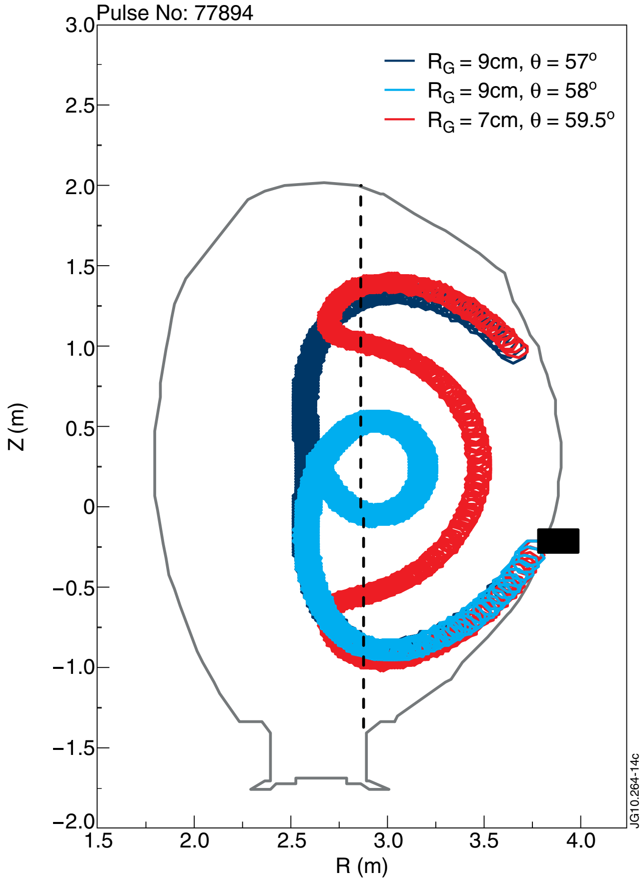

Figure 5: Orbits of lost H-ions calculated backward in time from (R_G, θ) coordinates on the scintillator related to the loss footprints in the Pulse No: 77894 (see Fig.4a); dash line – position of the resonance layer at 2.66T/1.75MA and f_{ICRH} = 42–42.5MHz

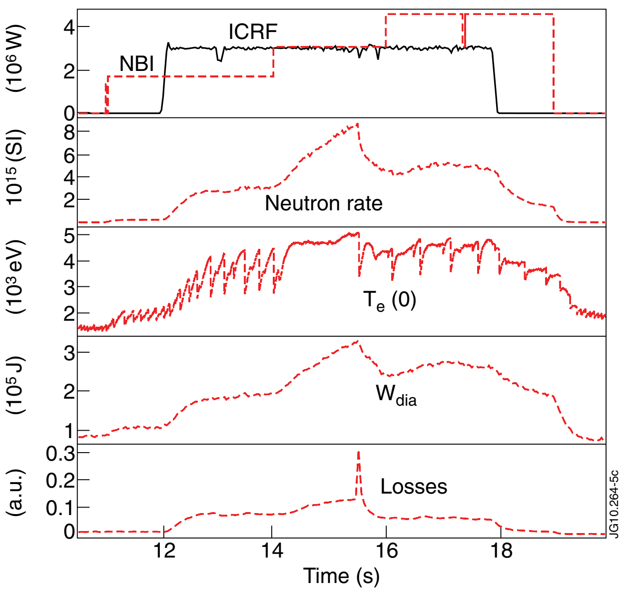

Figure 6: A typical JET D-plasma discharge 2.2T/ 2.2MA with 3rd harmonic ICRH (51MHz) of D beam-ions.

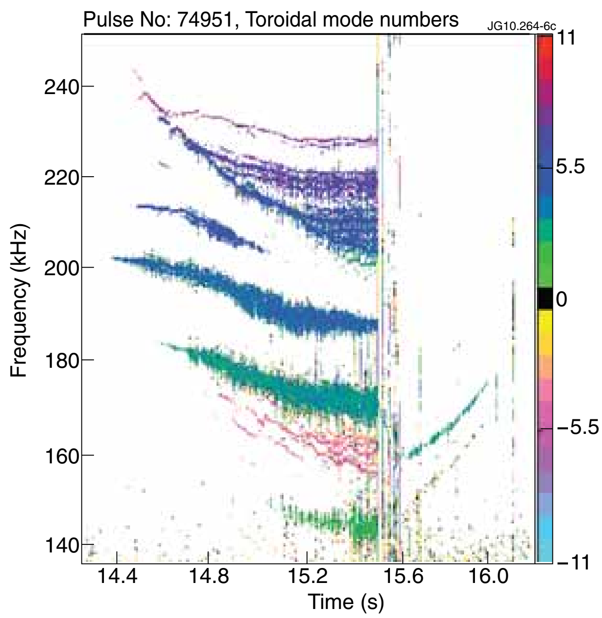

Figure 7: Magnetic spectrogram showing toroidal mode numbers of TAE and tornado modes before monster sawtooth crash in Pulse No's: 74951.

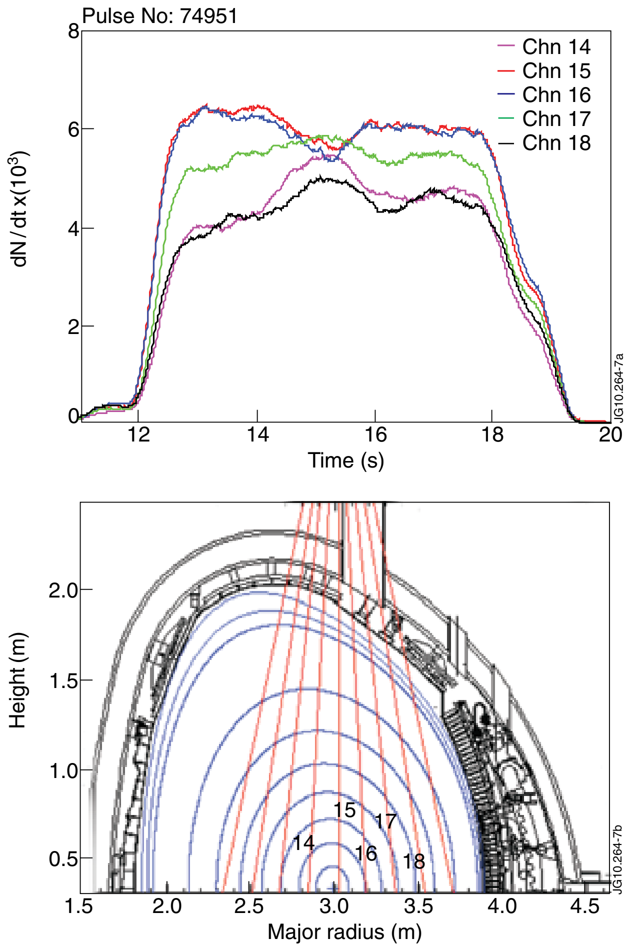

Figure 8: Top – 3.1MeV γ-ray intensities versus time recorded by vertical camera; bottom – the vertical camera lines of sight.